

# Experimental Assessment of the Relative Affinities of Benzene and Ferrocene toward the Li<sup>+</sup> Cation

Linda Kaufmann, Hannes Vitze, Michael Bolte, Hans-Wolfram Lerner, and Matthias Wagner\*

*Institut für Anorganische Chemie, J.W. Goethe-Universität Frankfurt, Max-von-Laue-Strasse 7, D-60438 Frankfurt (Main), Germany*

Received December 10, 2006

In order to explore whether benzene or ferrocene presents a more attractive  $\pi$  face to Li<sup>+</sup> ions, the lithium tetraorganylborate Li[BFC<sub>2</sub>Ph<sub>2</sub>] has been synthesized, which contains two phenyl rings as well as two ferrocenyl substituents as potential coordination sites (Fc = (C<sub>5</sub>H<sub>5</sub>)Fe(C<sub>5</sub>H<sub>4</sub>)). The compound crystallizes from toluene/dibutyl ether as the contact ion pair [Li(OBu<sub>2</sub>)]<sup>+</sup>[BFC<sub>2</sub>Ph<sub>2</sub>]<sup>-</sup>, with the Li<sup>+</sup> ion located between the two borylated ferrocenyl cyclopentadienyl rings. This finding indicates ferrocene to be a stronger Li<sup>+</sup> binder than benzene. In line with this conclusion, the hexaphenyl derivative [(Li(OBu<sub>2</sub>))<sub>2</sub>][1,1'-fc(BPh<sub>3</sub>)<sub>2</sub>] was found to have each of its cyclopentadienyl substituents coordinated to one Li<sup>+</sup> ion, thereby forming a multiple-decker sandwich complex in the solid state (fc = (C<sub>5</sub>H<sub>4</sub>)<sub>2</sub>Fe).

## Introduction

Metal cations are attracted to the  $\pi$  faces of aromatic systems through strong forces.<sup>1</sup> In the case of alkali-metal ions, this interaction is mainly electrostatic.<sup>2</sup> Today, about 25 years after gas-phase studies of ion–molecule complexes provided the first evidence for the existence of such an effect,<sup>3</sup> it is obvious that cation– $\pi$  interactions play a prominent role also in the condensed phase. Studies using cyclophane receptors in aqueous media have shown that a hydrophobic cavity comprised of aromatic moieties can compete successfully with full aqueous solvation in the binding of metal cations.<sup>4,5</sup> In line with that, it is nowadays widely accepted that cation– $\pi$  interactions are important for molecular recognition and catalysis not only in artificial but also in biological systems.<sup>1,6</sup>

Our interest in an investigation of cation– $\pi$  interactions was sparked by the serendipitous finding that ferrocene reacts with GaCl<sub>3</sub> in a redox reaction, giving [Fe(C<sub>5</sub>H<sub>5</sub>)<sub>2</sub>]<sup>+</sup>[GaCl<sub>4</sub>]<sup>-</sup> and [Fe(C<sub>5</sub>H<sub>5</sub>)<sub>2</sub>Ga]<sup>+</sup>[GaCl<sub>4</sub>]<sup>-</sup> (**1**; Figure 1).<sup>7</sup> An X-ray crystal structure analysis of **1** revealed polycationic multiple-decker sandwich complexes of ferrocene and Ga<sup>+</sup> ions, each of them coordinated to the Cp rings of two ferrocene molecules in an  $\eta^5$  fashion. It thus became evident that cation– $\pi$  interactions are not restricted to arene derivatives but may also include organometallic  $\pi$  systems. Most interestingly, the crystals of **1** were grown from a mother liquor containing substantial amounts of benzene, which is a well-established ligand in the coordina-

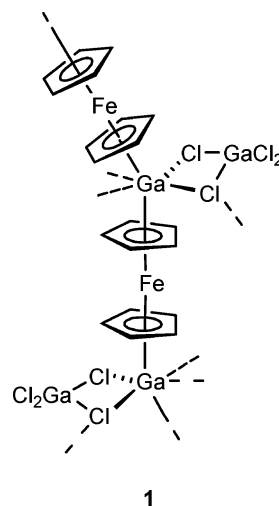


**Figure 1.** The ligand-unsupported Ga<sup>+</sup>–ferrocene multiple-decker sandwich complex **1**.

tion chemistry of Ga<sup>+</sup>.<sup>8,9</sup> Our experiment therefore suggested ferrocene to present an even more attractive  $\pi$  face to Ga<sup>+</sup> than benzene, an assumption that was further supported by quantum-chemical calculations.<sup>7</sup>

These results are intriguing in two respects. (i) Ferrocene-containing multiple-decker sandwich complexes represent a virtually unexplored class of compounds<sup>10–12</sup> which may be expected to possess very interesting electronic and optical properties. (ii) Information on cation– $\pi$  interactions with ferrocene as the  $\pi$  system is scarce.<sup>13,14</sup> Thus, if ferrocene

\* To whom correspondence should be addressed. Fax: +49 69 798 29260. E-mail: Matthias.Wagner@chemie.uni-frankfurt.de.

(1) Ma, J. C.; Dougherty, D. A. *Chem. Rev.* **1997**, *97*, 1303–1324.

(2) Gokel, G. W.; De Wall, S. L.; Meadows, E. S. *Eur. J. Org. Chem.* **2000**, 2967–2978.

(3) Sunner, J.; Nishizawa, K.; Kebarle, P. *J. Phys. Chem.* **1981**, *85*, 1814–1820.

(4) Gross, J.; Harder, G.; Vögtle, F.; Stephan, H.; Gloe, K. *Angew. Chem., Int. Ed. Engl.* **1995**, *34*, 481–484.

(5) Gross, J.; Harder, G.; Siepen, A.; Harren, J.; Vögtle, F.; Stephan, H.; Gloe, K.; Ahlers, B.; Cammann, K.; Rissanen, K. *Chem. Eur. J.* **1996**, *2*, 1585–1595.

(6) Dougherty, D. A. *Science* **1996**, *271*, 163–168.

(7) Scholz, S.; Green, J. C.; Lerner, H.-W.; Bolte, M.; Wagner, M. *Chem. Commun.* **2002**, 36–37.

(8) Schmidbaur, H.; Thewalt, U.; Zafiropoulos, T. *Organometallics* **1983**, *2*, 1550–1554.

(9) Schmidbaur, H.; Bublak, W.; Huber, B.; Müller, G. *Organometallics* **1986**, *5*, 1647–1651.

(10) Schildcrout, S. M. *J. Am. Chem. Soc.* **1973**, *95*, 3846–3849.

(11) Crespo, O.; Gimeno, M. C.; Jones, P. G.; Laguna, A.; Sarroca, C. *Chem. Commun.* **1998**, 1481–1482.

(12) Nagao, S.; Kato, A.; Nakajima, A.; Kaya, K. *J. Am. Chem. Soc.* **2000**, *122*, 4221–4222.

(13) Enders, M.; Ludwig, G.; Pritzkow, H. *Organometallics* **2002**, *21*, 3856–3859.

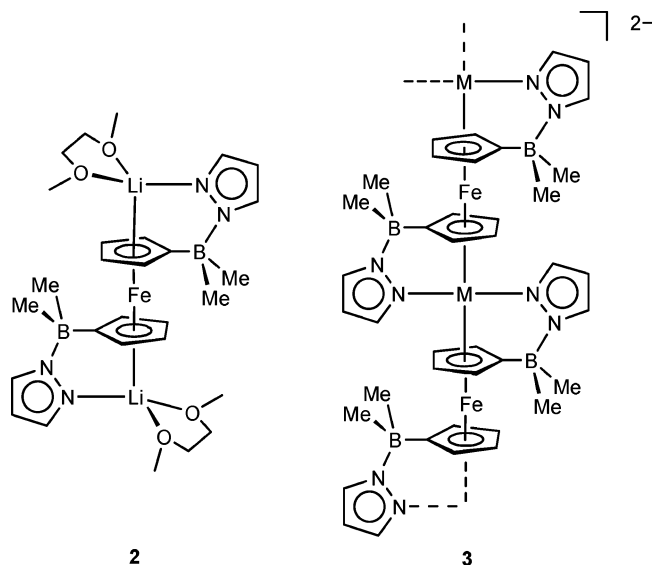


**Figure 2.** The ligand-supported alkali metal ion–ferrocene multiple-decker sandwich complexes **2** and **3** ( $M^+ = Na^+–Cs^+$ ; counterions and additional dimethoxyethane ligands omitted for clarity).

generally turned out to be superior to benzene for metal ion complexation, the design of ferrocene-based cyclophanes could lead to a new generation of artificial receptors possessing improved and redox-switchable cation affinities. It is worth noting that DFT calculations predict the binding enthalpies of  $M^+–\eta^5(\text{ferrocene})$  model complexes to be about 20% higher compared to those of the related  $M^+–\eta^6(\text{benzene})$  aggregates when  $M^+ = Li^+$ ,  $Na^+$ .<sup>15</sup> For  $K^+$  and  $Rb^+$ , the degree of cation– $\pi$  interaction with both aromatics is about the same.<sup>15</sup>

Given this background, our group has embarked on a systematic investigation of  $M^{n+}–\eta^5(\text{ferrocene})$  complexes. In our first series of targeted complexation studies we have employed the ditopic ferrocene-based mono(pyrazol-1-yl)borate ligand  $[1,1'-fc(\text{BMe}_2\text{pz})_2]^{2-}$  ( $fc = (\text{C}_5\text{H}_4)_2\text{Fe}$ ) and succeeded in the structural characterization of its  $Li^+–Cs^+$  multiple-decker sandwich complexes **2** and **3** (Figure 2).<sup>15</sup> The concept underlying this system is to attract the cation electrostatically to the ferrocene backbone and to stabilize it at a position above the Cp ring by means of the chelating pyrazolyl substituent.

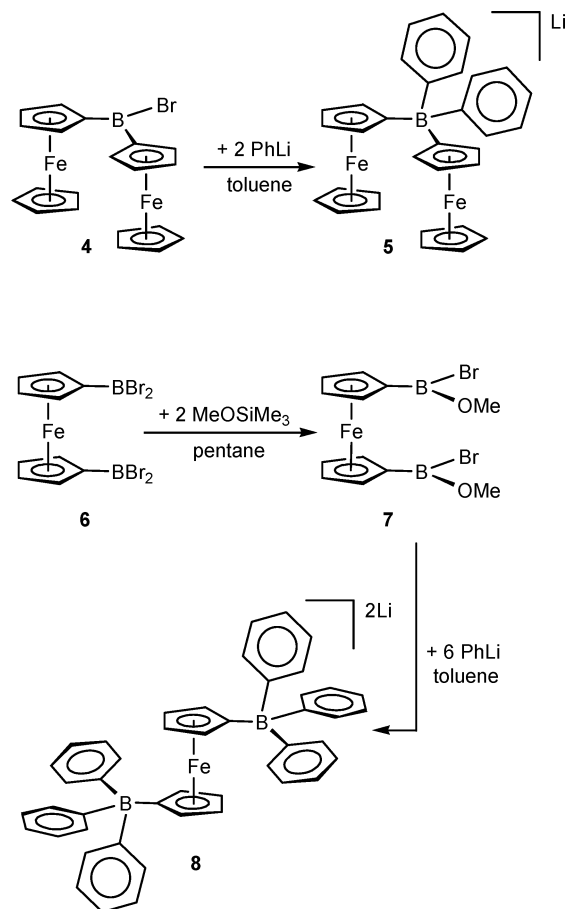
We will now show that it is possible to replace the Lewis basic pyrazolyl side arm of **2** by a simple phenyl ring without losing the desired  $Li^+–\eta^5(\text{ferrocene})$  contact. Moreover, we will describe a qualitative experimental evaluation of the relative affinities of benzene and ferrocene toward the  $Li^+$  cation.

## Results and Discussion

### Synthesis and NMR Spectroscopic Characterization.

In order to be able to compare the ligand properties of benzene and ferrocene under identical conditions, it is best to combine both moieties in the same molecule. We have chosen lithium diferrocenyldiphenylborate (**5**; Scheme 1) as our target compound for the following reasons. (i) The binding energies of alkali-metal ions  $M^+$  to aromatic  $\pi$  systems follow a classical

**Scheme 1.** Synthesis of the Lithium Tetraorganylborate Salts **5** and **8**



electrostatic trend and are thus largest in the case of  $M^+ = Li^+$ .<sup>1</sup> (ii) X-ray crystal structure analyses of the salts  $K[\text{BPh}_4]$ <sup>16</sup> and  $Rb[\text{BPh}_4]$ <sup>17</sup> show that the respective alkali-metal ion is embedded between two phenyl rings of the tetraphenylborate anion. For a similar chelating coordination mode in the case of **5**, the  $Li^+$  cation would have the choice between two phenyl rings, one phenyl and one ferrocenyl substituent, or two ferrocenyl groups.

Compound **5** was synthesized from  $\text{Fc}_2\text{BBR}_2$ <sup>18</sup> (**4**) and 2 equiv of  $\text{PhLi}$  (1.8 M solution in dibutyl ether) in toluene (Scheme 1). Single crystals of its dibutyl ether adduct **5**( $\text{OBu}_2$ ), which forms contact ion pairs in the solid state, were obtained from hot toluene. Single crystals of the corresponding solvent-separated ion pair **5**(12-crown-4)<sub>2</sub> were grown from a solution of **5**( $\text{OBu}_2$ ) and 12-crown-4 in THF at  $-35^\circ\text{C}$ .

The <sup>11</sup>B NMR spectrum of **5**( $\text{OBu}_2$ ) reveals one sharp resonance at  $-11.8$  ppm ( $h_{1/2} = 7$  Hz;  $d_8$ -THF), testifying to the presence of tetra-coordinate boron nuclei<sup>19</sup> (cf.  $\text{Na}[\text{BPh}_4]$  with  $\delta(^{11}\text{B}) -6.3$  ( $\text{CH}_3\text{CN}$ )<sup>20</sup> and  $\text{Li}[\text{BFc}_2\text{Me}_2]$  with  $\delta(^{11}\text{B}) -21.2$  ( $d_8$ -THF)<sup>18</sup>). In the <sup>1</sup>H NMR spectrum, three ferrocenyl resonances ( $\delta$  3.61, 3.87, 4.07), three phenyl resonances ( $\delta$  6.71, 6.85, 7.27), and four signals assignable to a dibutyl ether ligand

(16) Hoffmann, K.; Weiss, E. *J. Organomet. Chem.* **1974**, *67*, 221–228.

(17) Pajzderska, A.; Maluszyńska, H.; Wasicki, J. *Z. Naturforsch.* **2002**, *57a*, 847–853.

(18) Scheibitz, M.; Heilmann, J. B.; Winter, R. F.; Bolte, M.; Bats, J. W.; Wagner, M. *Dalton Trans.* **2005**, 159–170.

(19) Nöth, H.; Wrackmeyer, B. Nuclear Magnetic Resonance Spectroscopy of Boron Compounds. In *NMR Basic Principles and Progress*; Diehl, P., Fluck, E., Kosfeld, R., Eds.; Springer: Berlin, Heidelberg, New York, 1978.

(20) Nöth, H.; Vahrenkamp, H. *Chem. Ber.* **1966**, *99*, 1049–1067.

(14) Honeyman, G. W.; Kennedy, A. R.; Mulvey, R. E.; Sherrington, D. C. *Organometallics* **2004**, *23*, 1197–1199.

(15) Ilkhechi, A. H.; Mercero, J. M.; Silanes, I.; Bolte, M.; Scheibitz, M.; Lerner, H.-W.; Ugalde, J. M.; Wagner, M. *J. Am. Chem. Soc.* **2005**, *127*, 10656–10666.

**Table 1.** Selected Crystallographic Data for **5**(OBu<sub>2</sub>), **5**(12-crown-4)<sub>2</sub>, **7**, and **8**(OBu<sub>2</sub>)<sub>2</sub>

	<b>5</b> (OBu <sub>2</sub> )	<b>5</b> (12-crown-4) <sub>2</sub>	<b>7</b>	<b>8</b> (OBu <sub>2</sub> ) <sub>2</sub>
formula	C <sub>40</sub> H <sub>46</sub> BFe <sub>2</sub> LiO	C <sub>48</sub> H <sub>60</sub> BFe <sub>2</sub> LiO <sub>8</sub> ·C <sub>4</sub> H <sub>8</sub> O	C <sub>12</sub> H <sub>14</sub> B <sub>2</sub> Br <sub>2</sub> FeO <sub>2</sub>	C <sub>62</sub> H <sub>74</sub> B <sub>2</sub> FeLi <sub>2</sub> O <sub>2</sub>
fw	672.22	966.51	427.52	942.56
color, shape	orange, rod	orange, needle	orange–red, block	orange, block
temp (K)			173(2)	
radiation			Mo Kα, 0.710 73 Å	
cryst syst	orthorhombic	triclinic	monoclinic	orthorhombic
space group	<i>Pbca</i>	<i>P</i> $\bar{1}$	<i>P2</i> <sub>1</sub> / <i>c</i>	<i>P2</i> <sub>1</sub> <i>2</i> <sub>1</sub>
<i>a</i> (Å)	16.0743(11)	12.4841(9)	7.7169(8)	15.6422(13)
<i>b</i> (Å)	19.1000(9)	12.6561(10)	12.3681(9)	18.8747(14)
<i>c</i> (Å)	21.9454(11)	15.5274(14)	7.8101(7)	20.159(3)
α (deg)	90	86.595(7)	90	90
β (deg)	90	82.632(7)	101.294(8)	90
γ (deg)	90	87.525(6)	90	90
<i>V</i> (Å <sup>3</sup> )	6737.7(7)	2427.2(3)	730.99(11)	5951.8(10)
<i>Z</i>	8	2	2	4
<i>D</i> <sub>calcd</sub> (g cm <sup>-3</sup> )	1.325	1.322	1.942	1.052
<i>F</i> (000)	2832	1024	416	2016
μ (mm <sup>-1</sup> )	0.892	0.653	6.488	0.291
cryst size (mm <sup>3</sup> )	0.33 × 0.18 × 0.12	0.36 × 0.12 × 0.11	0.22 × 0.21 × 0.19	0.19 × 0.14 × 0.07
no. of rflns collected	38 071	25 348	11 861	21 935
no. of indep rflns ( <i>R</i> <sub>int</sub> )	6455 (0.0810)	9066 (0.0904)	1370 (0.0533)	10 819 (0.1079)
no. of data/restraints/params	6455/2/406	9066/0/586	1370/0/89	10 819/40/580
GOF on <i>F</i> <sup>2</sup>	0.927	0.962	1.112	1.101
<i>R</i> <sub>1</sub> , <i>wR</i> <sub>2</sub> ( <i>I</i> > 2σ( <i>I</i> ))	0.0633, 0.1083	0.0623, 0.1327	0.0275, 0.0642	0.1477, 0.3479
<i>R</i> <sub>1</sub> , <i>wR</i> <sub>2</sub> (all data)	0.1344, 0.1281	0.1113, 0.1524	0.0303, 0.0655	0.2460, 0.4106
largest diff peak, hole (e Å <sup>-3</sup> )	0.474, -0.649	1.018, -0.516	0.914, -0.590	1.063, -0.776

are observed with an overall integral ratio Fc:Ph:OBu<sub>2</sub> = 2:2:1. The corresponding <sup>13</sup>C NMR resonances all appear in the expected regions and thus do not merit further discussions. Signals of the ipso carbon atoms *i*-Ph and *i*-C<sub>5</sub>H<sub>4</sub> are broadened beyond detection, due to coupling with the quadrupolar boron nucleus. The <sup>7</sup>Li NMR spectrum of **5**(OBu<sub>2</sub>) is characterized by a resonance at -0.27 ppm (*d*<sub>8</sub>-THF). The chemical shift value δ(<sup>7</sup>Li) of **5**(12-crown-4)<sub>2</sub> is -0.32 ppm (*d*<sub>8</sub>-THF). Both values are typical for Li<sup>+</sup> cations surrounded by ether ligands. Thus, <sup>7</sup>Li NMR spectroscopy provides no evidence for Li<sup>+</sup>–ferrocenyl coordination in THF solution.

Compound **8** (Scheme 1) was prepared in order to prove not only that the multiple-decker compound **2** (Figure 2) is not merely an artifact of the structure-directing properties of the Lewis basic side arm but also that Li<sup>+</sup>–ferrocene π interactions indeed play an important role. Initial attempts to synthesize **8** directly from the diborylated ferrocene derivative 1,1'-fc(BBr<sub>2</sub>)<sub>2</sub> (**6**) and 6 equiv of PhLi resulted in a complex product mixture. We have therefore transformed **6** into the bromomethoxyborane **7** using MeOSiMe<sub>3</sub> in pentane. Subsequent reaction of **7** with PhLi (1.8 M solution in dibutyl ether) in toluene gave the lithium salt **8** in excellent yield. Single crystals of **8**(OBu<sub>2</sub>)<sub>2</sub> were grown from the reaction mixture at a temperature of -35 °C after LiBr and LiOMe had been removed. The <sup>11</sup>B NMR spectrum of **8**(OBu<sub>2</sub>)<sub>2</sub> is characterized by a single sharp resonance with a chemical shift value of -9.1 ppm (*h*<sub>1/2</sub> = 8 Hz). This leads to the conclusion that **8**(OBu<sub>2</sub>)<sub>2</sub> possesses a symmetric structure with magnetically equivalent boron sites. In line with that, the two cyclopentadienyl rings and the six phenyl substituents give rise to only two and three signals, respectively, in the <sup>1</sup>H as well as in the <sup>13</sup>C NMR spectrum (*i*-Ph and *i*-C<sub>5</sub>H<sub>4</sub> are again not visible due to quadrupolar broadening).

**X-ray Crystal Structure Determinations.** Details of the X-ray crystal structure analyses of the compounds **5**(OBu<sub>2</sub>), **5**(12-crown-4)<sub>2</sub>, **7**, and **8**(OBu<sub>2</sub>)<sub>2</sub> are summarized in Table 1. Plots of the molecular structures of **5**(OBu<sub>2</sub>), **5**(12-crown-4)<sub>2</sub>, and **8**(OBu<sub>2</sub>)<sub>2</sub> are shown in Figures 3–5; selected bond lengths and angles are compiled in the figure captions. For an ORTEP drawing of **7** and a description of its molecular structure, the reader is referred to the Supporting Information.

**5**(OBu<sub>2</sub>) crystallizes from toluene in the orthorhombic space group *Pbca* (Figure 3). The compound forms contact ion pairs in the solid state, with each Li<sup>+</sup> cation being coordinated by one dibutyl ether ligand (Li(1)–O(1) = 1.891(11) Å) and the substituted cyclopentadienyl rings of both ferrocenyl substitu-

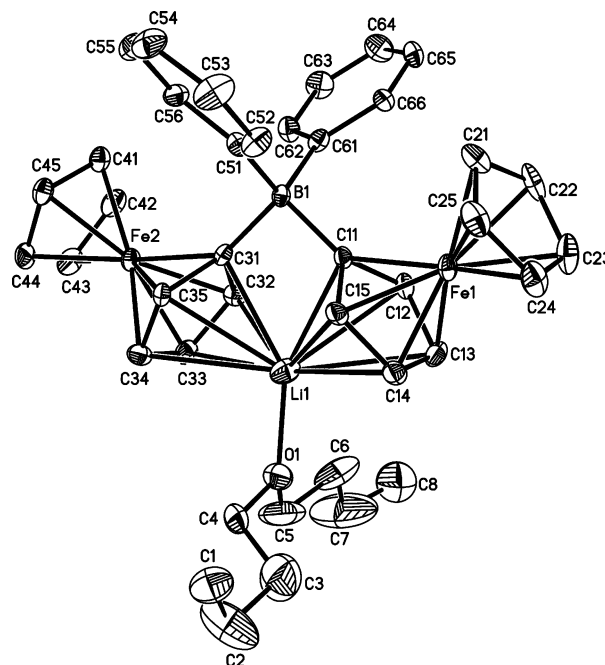


**Figure 3.** Structure of **5**(OBu<sub>2</sub>) in the crystal form. Thermal ellipsoids are drawn at the 30% probability level. H atoms are omitted for clarity. Selected bond lengths (Å), short contacts (Å), and bond angles (deg): Li(1)–O(1) = 1.891(11), B(1)–C(11) = 1.639(7), B(1)–C(31) = 1.642(7), B(1)–C(51) = 1.631(7), B(1)–C(61) = 1.643(7), Li(1)–C(11) = 2.397(11), Li(1)–C(15) = 2.316(11), Li(1)–C(31) = 2.415(10), Li(1)–C(32) = 2.372(10), Li(1)–COG(Cp(C11)) = 2.224, Li(1)–COG(Cp(C31)) = 2.231; C(11)–B(1)–C(31) = 98.1(4), C(51)–B(1)–C(61) = 109.6(4), COG(Cp(C11))–C(11)–B(1) = 166.5, COG(Cp(C31))–C(31)–B(1) = 165.6.

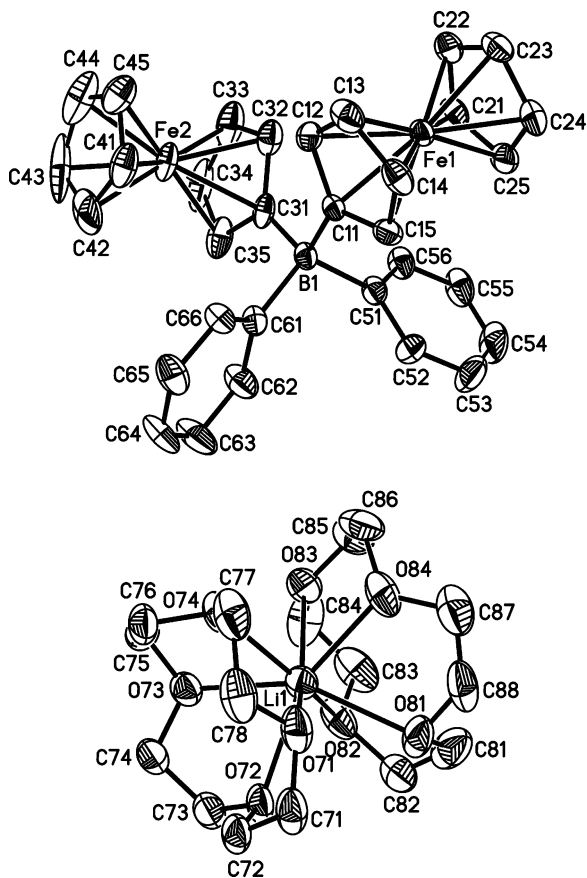


**Figure 4.** Structure of  $5(12\text{-crown-}4)_2$  in the crystal form. Thermal ellipsoids are drawn at the 50% probability level. H atoms are omitted for clarity. Selected bond lengths (Å) and bond angles (deg): B(1)–C(11) = 1.633(6), B(1)–C(31) = 1.637(6), B(1)–C(51) = 1.664(5), B(1)–C(61) = 1.651(6); C(11)–B(1)–C(31) = 113.7(3), C(51)–B(1)–C(61) = 109.3(3), COG(Cp(C11))–C(11)–B(1) = 173.8, COG(Cp(C31))–C(31)–B(1) = 175.7.

ents.<sup>21</sup> The distances between the Li<sup>+</sup> ion and the centers of gravity (COG) of the ferrocenyl cyclopentadienyl rings amount to Li(1)–COG(Cp(C11)) = 2.224 Å and Li(1)–COG(Cp(C31)) = 2.231 Å. They are thus longer than the corresponding calculated distances in the model complexes [Li<sup>+</sup>– $\eta^5$ -(C<sub>5</sub>H<sub>5</sub>)–Fe(C<sub>5</sub>H<sub>5</sub>)] (Li–COG = 1.870 Å) and [Li<sup>+</sup>–{ $\eta^5$ -(C<sub>5</sub>H<sub>5</sub>)Fe(C<sub>5</sub>H<sub>5</sub>)}<sub>2</sub>] (Li–COG = 1.995 Å).<sup>15,22</sup> It has, however, to be taken into account that solid-state structures are compared with gas-phase structures. Moreover, the Li–COG distances observed for  $5(\text{OBu}_2)_2$  compare well with the corresponding contacts in the solid-state structure of **2** (Li(1)–COG(1) = 2.26 Å, Li(2)–COG(2) = 2.32 Å).<sup>15,23</sup> All Li–C distances in  $5(\text{OBu}_2)_2$  fall in the range between 2.316(11) and 2.751(12) Å, with the shortest contacts being established to C(15) and C(32) (Li(1)–C(15) = 2.316(11) Å, Li(1)–C(32) = 2.372(10) Å) as well as to the ipso carbon atoms (Li(1)–C(11) = 2.397(11) Å, Li(1)–C(31) = 2.415(10) Å). Most interestingly, the molecular framework of the tetraorganylborate anion suffers from characteristic distortions improving the Li<sup>+</sup>–ferrocenyl interaction. (i) The bond angle spanned by the ferrocenyl ipso carbon atoms and the boron bridge (C(11)–B(1)–C(31) = 98.1(4)°) is signifi-

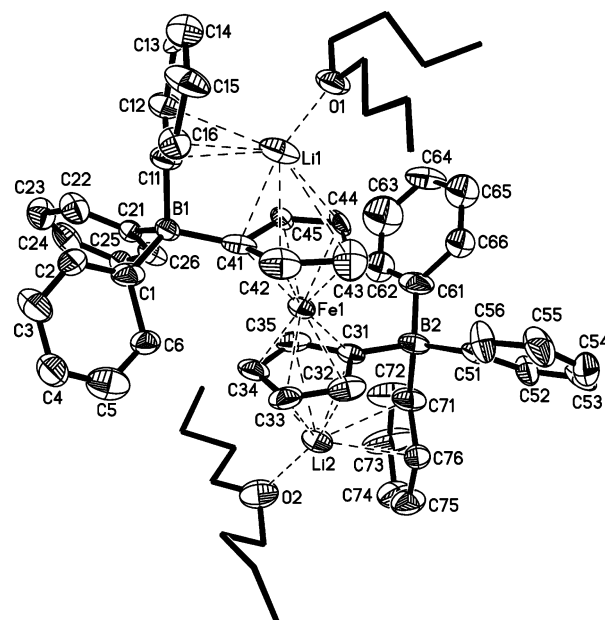


**Figure 5.** Structure of  $8(\text{OBu}_2)_2$  in the crystal form. Thermal ellipsoids are drawn at the 30% probability level. H atoms are omitted for clarity; butyl chains are shown as sticks. Selected bond lengths (Å), short contacts (Å), and bond angles (deg): Li(1)–O(1) = 1.86(2), Li(2)–O(2) = 1.88(2), B(1)–C(41) = 1.580(18), B(2)–C(31) = 1.73(2), Li(1)–C(11) = 2.42(3), Li(1)–C(41) = 2.311(19), Li(2)–C(31) = 2.305(19), Li(2)–C(76) = 2.42(3), Li(1)–COG(Cp(C41)) = 2.16, Li(2)–COG(Cp(C31)) = 2.15; C(11)–B(1)–C(41) = 102.0(8), C(31)–B(2)–C(71) = 100.1(10).

cantly smaller than the bond angle between the boron atom and the phenyl ipso carbon atoms (C(51)–B(1)–C(61) = 109.6(4)°). (ii) The two cyclopentadienyl rings are bent toward the Li<sup>+</sup> ion by angles COG(Cp(C11))–C(11)–B(1) and COG(Cp(C31))–C(31)–B(1) of 166.5 and 165.6°, respectively. Importantly, the corresponding angles in the solvent-separated ion pair  $5(12\text{-crown-}4)_2$  (triclinic, *P*1; Figure 4) are much closer to the ideal values of 109.5 and 180°, respectively (cf. C(11)–B(1)–C(31) = 113.7(3)°, COG(Cp(C11))–C(11)–B(1) = 173.8°, COG(Cp(C31))–C(31)–B(1) = 175.7°).

$8(\text{OBu}_2)_2$  (orthorhombic, space group *P*2<sub>1</sub>2<sub>1</sub>2<sub>1</sub>) also forms contact ion pairs in the solid state (Figure 5). The two Li<sup>+</sup> ions, each of them bearing one dibutyl ether ligand, are located above the two cyclopentadienyl rings with distances Li(1)–COG(Cp(C41)) = 2.16 Å and Li(2)–COG(Cp(C31)) = 2.15 Å. These values are smaller than in  $5(\text{OBu}_2)_2$  and the pyrazolyl-containing analogue **2** and compare well with the Li–COG distance of 2.018 Å calculated for [Li<sup>+</sup>– $\eta^5$ -(C<sub>5</sub>H<sub>5</sub>)Fe(C<sub>5</sub>H<sub>5</sub>)– $\eta^5$ –Li<sup>+</sup>].<sup>15</sup> The structure is further stabilized by  $\pi$  interactions between each Li<sup>+</sup> ion and one of its three adjacent phenyl substituents. However, the shortest Li–phenyl distances (Li(1)–C(11) = Li(2)–C(76) = 2.42(3) Å) are longer than the shortest Li–ferrocenyl contacts (Li(1)–C(41) = 2.311(19) Å, Li(2)–C(31) = 2.305(19) Å). Similar to the case for  $5(\text{OBu}_2)_2$ ,  $8(\text{OBu}_2)_2$  features rather small bond angles, C(11)–B(1)–C(41) = 102.0(8)° and C(31)–B(2)–C(71) = 100.1(10)°, as a result of the chelating coordination mode of the anionic moiety.

**Electrochemical Investigations.** Table 2 summarizes the electrochemical parameters of the redox events exhibited by  $5(\text{OBu}_2)_2$ ,  $8(\text{OBu}_2)_2$ , and the related complexes Li[BFC<sub>2</sub>Me<sub>2</sub>]<sup>18</sup> and Li<sub>2</sub>[Fc–BMe<sub>2</sub>–fc–BMe<sub>2</sub>–Fc]; supporting electrolyte: [NBu<sub>4</sub>][PF<sub>6</sub>].<sup>18</sup> Since Li[BFC<sub>2</sub>Me<sub>2</sub>] and Li<sub>2</sub>[Fc–BMe<sub>2</sub>–fc–BMe<sub>2</sub>–Fc] tend to decompose upon oxidation at room temperature, they had to

(21) We have investigated the bulk material of  $5(\text{OBu}_2)_2$  using X-ray powder diffractometry and found the single crystal to be representative for the entire sample.

(22) Irigoras, A.; Mercero, J. M.; Silanes, I.; Ugalde, J. M. *J. Am. Chem. Soc.* **2001**, *123*, 5040–5043.

(23) Ilkhechi, A. H.; Scheibitz, M.; Bolte, M.; Lerner, H.-W.; Wagner, M. *Polyhedron* **2004**, *23*, 2597–2604.



**Table 2. Formal Electrode Potentials  $E_{1/2}$  (vs FcH/FcH<sup>+</sup>) and Peak-to-Peak Separations  $\Delta E$  (at 0.1 V s<sup>-1</sup>) for the Fe(II)/Fe(III) Redox Changes Exhibited by Compounds **5**(OBu<sub>2</sub>), **8**(OBu<sub>2</sub>)<sub>2</sub>, Li[BFC<sub>2</sub>Me<sub>2</sub>],<sup>18</sup> and Li<sub>2</sub>[Fc-BMe<sub>2</sub>-fc-BMe<sub>2</sub>-Fc]<sup>18</sup>**

	$E_{1/2}$ (V)	$\Delta E$ (mV)	$\Delta E_{1/2}$ (mV)	$T$ (°C)	solvent	$\Delta E(\text{FcH})$ (mV)
<b>5</b> (OBu <sub>2</sub> )	-0.38/-0.64	99/97	260	20	CH <sub>2</sub> Cl <sub>2</sub>	103
<b>5</b> (OBu <sub>2</sub> )	-0.35/-0.57	102/112	220	-78	CH <sub>2</sub> Cl <sub>2</sub>	106
<b>8</b> (OBu <sub>2</sub> ) <sub>2</sub>	-1.09	97	20	20	CH <sub>2</sub> Cl <sub>2</sub>	111
<b>8</b> (OBu <sub>2</sub> ) <sub>2</sub>	-0.98	212		-78	CH <sub>2</sub> Cl <sub>2</sub>	122
Li[BFC <sub>2</sub> Me <sub>2</sub> ] <sup>a</sup>	-0.43/-0.64	90/100	210	-78	CH <sub>2</sub> Cl <sub>2</sub>	100
Li <sub>2</sub> [Fc-BMe <sub>2</sub> -fc-BMe <sub>2</sub> -Fc] <sup>a</sup>	-0.51/-1.21	330/210		-78	CH <sub>2</sub> Cl <sub>2</sub>	250

<sup>a</sup> Recorded at a scan rate of 0.2 V s<sup>-1</sup>.

be investigated at -78 °C. For reasons of comparison, the cyclic voltammograms of **5**(OBu<sub>2</sub>) and **8**(OBu<sub>2</sub>)<sub>2</sub> were also recorded at this temperature.

The dinuclear complex **5**(OBu<sub>2</sub>) displays two oxidation processes of relative intensity 1:1, assignable to successive one-electron transitions at the two ferrocenyl moieties (Figure 6a). These transitions are chemically reversible, as evidenced by the following criteria: the current ratios  $i_{p,c}/i_{p,a}$  are constantly equal to 1, the current functions  $i_{p,a}/v^{1/2}$  remain constant, and the peak-to-peak separations ( $\Delta E$ ) do not depart appreciably from the value found for the internal ferrocene standard ( $\Delta E(\text{FcH})$ , Table 2; the theoretically expected value for a chemically and electrochemically reversible one-electron step is 59 mV). Both  $E_{1/2}$  values of **5**(OBu<sub>2</sub>) (-0.35/-0.57 V) are slightly more anodically shifted than the redox potentials of Li[BFC<sub>2</sub>Me<sub>2</sub>] (-0.43/-0.64 V; Table 2), which can easily be explained by the greater electronegativity of the phenyl rings as compared to methyl substituents. The differences, however, between the redox potentials of the two Fe(II)/Fe(III) transitions are roughly the same in **5**(OBu<sub>2</sub>) ( $\Delta E_{1/2} = 220$  mV) and Li[BFC<sub>2</sub>Me<sub>2</sub>] ( $\Delta E_{1/2} = 210$  mV). These comparatively large  $\Delta E_{1/2}$  values indicate that an electronic communication between the two ferrocenyl moieties is possible via a tetracoordinated boron linker. In contrast to the methyl derivative Li[BFC<sub>2</sub>Me<sub>2</sub>], the phenyl-substituted compound **5**(OBu<sub>2</sub>) undergoes a reversible two-electron oxidation even at room temperature. We note an increase of  $\Delta E_{1/2}$  to a value of 260 mV under these conditions (Figure 6a).

The Fe(II)/Fe(III) redox transition exhibited by the dianionic salt **8**(OBu<sub>2</sub>)<sub>2</sub> shows features of chemical reversibility on the cyclic voltammetric time scale, both at -78 °C and at room temperature (Figure 6b). The corresponding potential values  $E_{1/2} = -0.98$  V (-78 °C), -1.09 V (room temperature) are extremely shifted into the cathodic regime. A similar value has been observed for the central ferrocenylene unit in Li<sub>2</sub>[Fc-BMe<sub>2</sub>-fc-BMe<sub>2</sub>-Fc], which is oxidized at  $E_{1/2} = -1.21$  V (Table 2). The effect of two tetraorganylborate substituents on the electrochemical properties of the ferrocene backbone is considerably larger than that of 10 methyl groups, since decamethylferrocene possesses a formal electrode potential of  $E_{1/2} = -0.55$  V vs the FcH/FcH<sup>+</sup> couple (CH<sub>2</sub>Cl<sub>2</sub>; [NBu<sub>4</sub>][PF<sub>6</sub>]).

## Conclusion

The solid-state structure of the lithium tetraorganylborate salt [Li(OBu<sub>2</sub>)][BFC<sub>2</sub>Ph<sub>2</sub>] (**5**(OBu<sub>2</sub>)) shows a contact ion pair with the Li<sup>+</sup> cation being chelated by the  $\pi$  faces of the two substituted cyclopentadienyl rings (distances between Li<sup>+</sup> and the centers of gravity (COG) of the cyclopentadienyl rings: 2.224, 2.231 Å). Since a similar structural motif with chelating phenyl substituents would also be possible, our results suggest

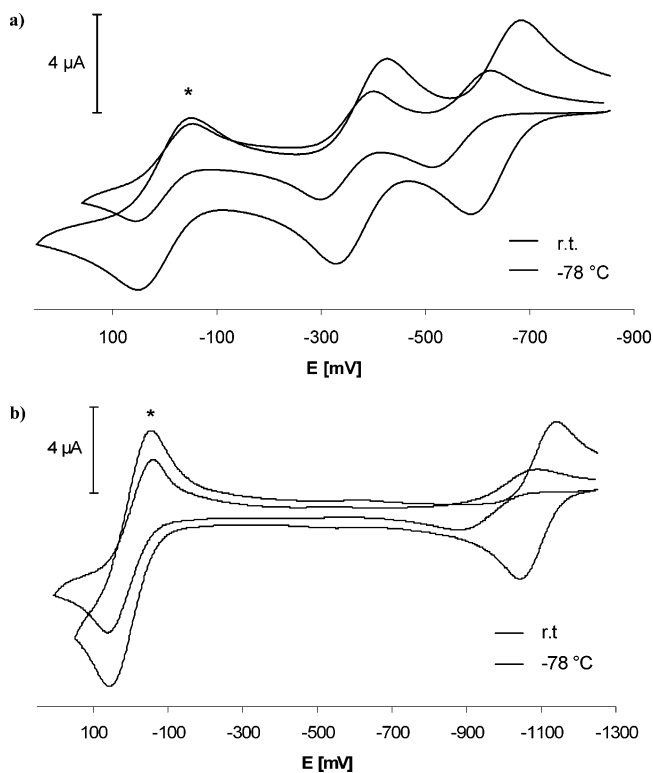


**Figure 6.** Cyclic voltammograms recorded at a platinum-disk electrode (i.d. 2 mm) on CH<sub>2</sub>Cl<sub>2</sub> solutions containing [NBu<sub>4</sub>][PF<sub>6</sub>] (0.1 mol l<sup>-1</sup>), referenced against the FcH/FcH<sup>+</sup> couple (marked with asterisks): (a) **5**(OBu<sub>2</sub>); (b) **8**(OBu<sub>2</sub>)<sub>2</sub>.

that the affinity of Li<sup>+</sup> toward ferrocene is higher than that toward benzene. In line with that, the lithium salt of the dianion [1,1'-fc(BPh<sub>3</sub>)<sub>2</sub>]<sup>2-</sup> (**8**(OBu<sub>2</sub>)<sub>2</sub>) exists as a multiple-decker sandwich complex in the crystal lattice (Li-COG = 2.15, 2.16 Å).

Both **5**(OBu<sub>2</sub>) and **8**(OBu<sub>2</sub>)<sub>2</sub> show reversible Fe(II)/Fe(III) redox transitions on the cyclic voltammetric time scale. The corresponding formal electrode potentials are strongly shifted into the cathodic regime as a result of the presence of one and two tetraorganylborate substituents (**5**(OBu<sub>2</sub>),  $E_{1/2} = -0.38/-0.64$  V; **8**(OBu<sub>2</sub>)<sub>2</sub>,  $E_{1/2} = -1.09$  V; room temperature). The difference  $\Delta E_{1/2}$  of 260 mV between the two redox waves in the cyclic voltammogram of **5**(OBu<sub>2</sub>) points toward a significant electronic communication of the two ferrocenyl substituents in this molecule. Our results are relevant for future research, because they (i) indicate that even more efficient host molecules for cation complexation could be developed by substitution of ferrocene moieties for the phenylene rings in cyclophane receptors, (ii) suggest a path for the assembly of ferrocene-based multiple-decker sandwich complexes by introducing anionic tetraorganylborate substituents, and (iii) provide conclusive evidence for the fact that boranediyl-bridged oligo-(ferrocenylenes) [-fc-BR<sub>2</sub>]<sub>n</sub><sup>18,24,25</sup> gain more stability from aryl than from alkyl substituents R.

## Experimental Section

**General Remarks.** All reactions were carried out under a nitrogen atmosphere using Schlenk tube techniques. Solvents were freshly distilled under argon from Na/benzophenone (toluene, C<sub>6</sub>D<sub>6</sub>,

(24) Scheibitz, M.; Winter, R. F.; Bolte, M.; Lerner, H.-W.; Wagner, M. *Angew. Chem., Int. Ed.* **2003**, *42*, 924–927.

(25) Heilmann, J. B.; Scheibitz, M.; Qin, Y.; Sundaraman, A.; Jäkle, F.; Kretz, T.; Bolte, M.; Lerner, H.-W.; Holthausen, M. C.; Wagner, M. *Angew. Chem., Int. Ed.* **2006**, *45*, 920–925.

THF, *d*<sub>8</sub>-THF), Na/Pb alloy (hexane, pentane), or CaH<sub>2</sub> (CH<sub>2</sub>Cl<sub>2</sub>) prior to use. NMR: Bruker AM 250 and Avance 400. Chemical shifts are referenced to residual solvent peaks (<sup>1</sup>H, <sup>13</sup>C{<sup>1</sup>H}) or external BF<sub>3</sub>·Et<sub>2</sub>O (<sup>11</sup>B{<sup>1</sup>H}). Abbreviations: tr = triplet, vtr = virtual triplet, vquin = virtual quintet, vsex = virtual sextet, mult = multiplet, br = broad, n.o. = signal not observed, *i* = ipso, *o* = ortho, *m* = meta, *p* = para. Electrochemical measurements: potentiostat EG&G Princeton Applied Research 263 A.

**Synthesis of 5.** A solution of PhLi in dibutyl ether (1.8 M; 0.63 mL, 1.13 mmol) was diluted with toluene (8 mL) and added dropwise with stirring at −78 °C to a solution of Fc<sub>2</sub>BBr (**4**; 0.26 g, 0.56 mmol) in toluene (12 mL). The reaction mixture was slowly warmed to room temperature and stirred overnight. The resulting orange suspension was heated to reflux temperature and quickly filtered while still hot. Orange single crystals of **5**(OBu<sub>2</sub>) formed from the filtrate upon cooling to room temperature. Yield of single crystalline **5**(OBu<sub>2</sub>): 0.16 g (43%). To a solution of **5**(OBu<sub>2</sub>) (0.010 g, 0.015 mmol) in THF (2 mL) was added one drop of 12-crown-4. The resulting solution was stored at −35 °C for 3 days to give single crystals of **5**(12-crown-4)<sub>2</sub>. NMR data for **5**(OBu<sub>2</sub>): <sup>11</sup>B{<sup>1</sup>H} NMR (128.4 MHz, *d*<sub>8</sub>-THF, 303 K) δ −11.8 (*h*<sub>1/2</sub> = 7 Hz); <sup>7</sup>Li{<sup>1</sup>H} NMR (155.5 MHz, *d*<sub>8</sub>-THF, 303 K) δ −0.27 (*h*<sub>1/2</sub> = 1 Hz); <sup>1</sup>H NMR (400.1 MHz, *d*<sub>8</sub>-THF, 303 K) δ 0.91 (tr, 6H, <sup>3</sup>J<sub>HH</sub> = 7.3 Hz, CH<sub>3</sub>), 1.37 (vsex, 4H, <sup>3</sup>J<sub>HH</sub> = 7.4 Hz, CH<sub>2</sub>CH<sub>3</sub>), 1.50 (vquin, 4H, <sup>3</sup>J<sub>HH</sub> = 6.9 Hz, OCH<sub>2</sub>CH<sub>2</sub>), 3.35 (tr, 4H, <sup>3</sup>J<sub>HH</sub> = 6.4 Hz, OCH<sub>2</sub>), 3.61 (s, 10H, C<sub>5</sub>H<sub>5</sub>), 3.87, 4.07 (1 × vtr, br, 2 × 4H, <sup>3</sup>J<sub>HH</sub> = <sup>4</sup>J<sub>HH</sub> = 1.5 Hz, C<sub>5</sub>H<sub>4</sub>), 6.71 (tr, 2H, <sup>3</sup>J<sub>HH</sub> = 7.1 Hz, *p*-Ph), 6.85 (vtr, 4H, <sup>3</sup>J<sub>HH</sub> = 7.4 Hz, *m*-Ph), 7.27 (mult, 4H, *o*-Ph); <sup>13</sup>C{<sup>1</sup>H} NMR (100.6 MHz, *d*<sub>8</sub>-THF, 303 K) δ 14.5 (CH<sub>3</sub>), 20.5 (CH<sub>2</sub>CH<sub>3</sub>), 33.1 (OCH<sub>2</sub>CH<sub>2</sub>), 67.1 (C<sub>5</sub>H<sub>4</sub>), 68.2 (C<sub>5</sub>H<sub>5</sub>), 71.3 (OCH<sub>2</sub>), 75.0 (C<sub>5</sub>H<sub>4</sub>), 121.7 (*p*-Ph), 125.2 (*m*-Ph), 136.7 (*o*-Ph), n.o. (*i*-C<sub>5</sub>H<sub>4</sub>, *i*-Ph). The NMR data of the anionic moieties [BFc<sub>2</sub>Ph<sub>2</sub>]<sup>−</sup> in *d*<sub>8</sub>-THF are identical for **5**(OBu<sub>2</sub>) and **5**(12-crown-4)<sub>2</sub>. Anal. Calcd for C<sub>32</sub>H<sub>28</sub>·BF<sub>2</sub>Li (541.99)·OC<sub>8</sub>H<sub>18</sub> (130.23): C, 71.47; H, 6.90. Found: C, 71.47; H, 6.83.

**Synthesis of 7.** A solution of MeOSiMe<sub>3</sub> (1.21 g, 11.61 mmol) in pentane (5 mL) was added dropwise at −78 °C to a suspension of 1,1'-fc(BBr<sub>2</sub>)<sub>2</sub> (**6**; 3.05 g, 5.81 mmol) in pentane (20 mL). The reaction mixture was slowly warmed to rt and stirred overnight, whereupon an orange solid precipitated. All volatiles were removed from the reaction mixture in vacuo and the crude solid product recrystallized from hexane. Yield: 2.43 g (98%). <sup>11</sup>B{<sup>1</sup>H} NMR (128.4 MHz, C<sub>6</sub>D<sub>6</sub>, 303 K): δ 39.3 (*h*<sub>1/2</sub> = 200 Hz). <sup>1</sup>H NMR (400.1 MHz, C<sub>6</sub>D<sub>6</sub>, 303 K): δ 3.57 (s, 6H, CH<sub>3</sub>), 4.27, 4.57 (2 × vtr, 2 × 4H, <sup>3</sup>J<sub>HH</sub> = <sup>4</sup>J<sub>HH</sub> = 1.8 Hz, C<sub>5</sub>H<sub>4</sub>). <sup>13</sup>C{<sup>1</sup>H} NMR (100.6 MHz, C<sub>6</sub>D<sub>6</sub>, 303 K): δ 56.8 (CH<sub>3</sub>), 74.7, 76.2 (C<sub>5</sub>H<sub>4</sub>).

**Synthesis of 8.** A solution of PhLi in dibutyl ether (1.8 M; 1.72 mL, 3.10 mmol) was diluted with toluene (8 mL) and added dropwise with stirring at −78 °C to a solution of 1,1'-fc(B(OMe)-Br)<sub>2</sub> (**7**; 0.22 g, 0.51 mmol) in toluene (12 mL). The reaction mixture was slowly warmed to room temperature and stirred overnight. The resulting brown suspension was filtered and the filtrate stored at −35 °C. After 3 days, orange single crystals of **8**(OBu<sub>2</sub>)<sub>2</sub> had formed. Yield: 0.42 g (87%). <sup>11</sup>B{<sup>1</sup>H} NMR (128.4 MHz, *d*<sub>8</sub>-THF, 303 K): δ −9.1 (*h*<sub>1/2</sub> = 8 Hz). <sup>7</sup>Li{<sup>1</sup>H} NMR (155.5 MHz, *d*<sub>8</sub>-THF, 303 K): δ −0.52 (*h*<sub>1/2</sub> = 1 Hz). <sup>1</sup>H NMR (400.1 MHz, *d*<sub>8</sub>-THF, 303 K): δ 0.91 (tr, 12H, <sup>3</sup>J<sub>HH</sub> = 7.3 Hz, CH<sub>3</sub>), 1.37

(vsex, 8H, <sup>3</sup>J<sub>HH</sub> = 7.4 Hz, CH<sub>2</sub>CH<sub>3</sub>), 1.51 (vquin, 8H, <sup>3</sup>J<sub>HH</sub> = 6.9 Hz, OCH<sub>2</sub>CH<sub>2</sub>), 3.35 (tr, 8H, <sup>3</sup>J<sub>HH</sub> = 6.2 Hz, OCH<sub>2</sub>), 3.47, 3.60 (2 × br, 2 × 4H, C<sub>5</sub>H<sub>4</sub>), 6.66 (tr, 6H, <sup>3</sup>J<sub>HH</sub> = 7.0 Hz, *p*-Ph), 6.81 (vtr, 12H, <sup>3</sup>J<sub>HH</sub> = 7.4 Hz, *m*-Ph), 7.41 (mult, 12H, *o*-Ph). <sup>13</sup>C{<sup>1</sup>H} NMR (100.6 MHz, *d*<sub>8</sub>-THF, 303 K): δ 14.5 (CH<sub>3</sub>), 20.5 (CH<sub>2</sub>CH<sub>3</sub>), 33.1 (OCH<sub>2</sub>CH<sub>2</sub>), 69.4 (br, C<sub>5</sub>H<sub>4</sub>), 71.3 (OCH<sub>2</sub>), 75.0 (br, C<sub>5</sub>H<sub>4</sub>), 121.4 (*p*-Ph), 125.3 (*m*-Ph), 137.2 (*o*-Ph), n.o. (*i*-C<sub>5</sub>H<sub>4</sub>, *i*-Ph). Anal. Calcd for C<sub>46</sub>H<sub>38</sub>B<sub>2</sub>FeLi<sub>2</sub> (682.10)·2OC<sub>8</sub>H<sub>18</sub> (260.46): C, 79.00; H, 7.91. Found: C, 78.55; H, 7.90.

**X-ray Crystal Structure Analysis of 5(OBu<sub>2</sub>), 5(12-crown-4)<sub>2</sub>, 7, and 8(OBu<sub>2</sub>)<sub>2</sub>.** Single crystals of **5**(OBu<sub>2</sub>) (orange rod, 0.33 × 0.18 × 0.12 mm), **5**(12-crown-4)<sub>2</sub> (orange needle, 0.36 × 0.12 × 0.11 mm), **7** (orange-red block, 0.22 × 0.21 × 0.19 mm), and **8**(OBu<sub>2</sub>)<sub>2</sub> (orange block, 0.19 × 0.14 × 0.07 mm) were analyzed with a STOE IPDS II two-circle diffractometer with graphite-monochromated Mo Kα radiation. Empirical absorption corrections were performed using the MULABS<sup>26</sup> option in PLATON;<sup>27</sup> the minimum and maximum transmissions were 0.7574/0.9005 (**5**(OBu<sub>2</sub>)), 0.7990/0.9317 (**5**(12-crown-4)<sub>2</sub>), 0.3294/0.3720 (**7**), and 0.9468/0.9799 (**8**(OBu<sub>2</sub>)<sub>2</sub>). The structures were solved by direct methods using the program SHELXS<sup>28</sup> and refined against *F*<sup>2</sup> with full-matrix least-squares techniques using the program SHELXL-97.<sup>29</sup> Most non-hydrogen atoms were refined with anisotropic displacement parameters (exceptions: disordered methyl group in **5**(OBu<sub>2</sub>); atoms of the disordered phenyl ring and C atoms of one dibutyl ether molecule in **8**(OBu<sub>2</sub>)<sub>2</sub>). Hydrogen atoms were refined using a riding model. One methyl group of the dibutyl ether ligand in **5**(OBu<sub>2</sub>) is disordered over two positions, which could be refined (occupancy factors 0.72(2) and 0.28(2)); the C–C bond lengths involving this disordered methyl group were refined with a distance restraint of 1.50(1) Å. The crystals of **5**(12-crown-4)<sub>2</sub> contain 1 equiv of THF. The crystal of **8**(OBu<sub>2</sub>)<sub>2</sub> was an inversion twin with a ratio of the twin components of 0.45(6)/0.55(6). Thus, the absolute structure could not be determined. One phenyl substituent of **8**(OBu<sub>2</sub>)<sub>2</sub> is disordered over two positions (occupancy factors 0.63(2) and 0.37(2)). Several restraints had to be applied in order to keep the geometric parameters of the disordered atoms in a reasonable range. CCDC reference numbers: 621902 (**5**(OBu<sub>2</sub>)), 634040 (**5**(12-crown-4)<sub>2</sub>), 629323 (**7**), 621903 (**8**(OBu<sub>2</sub>)<sub>2</sub>).

**Acknowledgment.** M.W. is grateful to the “Deutsche Forschungsgemeinschaft” (DFG) and the “Fonds der Chemischen Industrie” (FCI) for financial support. L.K. wishes to thank the “Hessisches Ministerium für Wissenschaft und Kunst” for a Ph.D. grant.

**Supporting Information Available:** CIF files giving crystallographic data for **5**(OBu<sub>2</sub>), **5**(12-crown-4)<sub>2</sub>, **7**, and **8**(OBu<sub>2</sub>)<sub>2</sub> and a figure giving an ORTEP drawing of **7** and description of its molecular structure. This material is available free of charge via the Internet at <http://pubs.acs.org>.

OM061117K

(26) Blessing, R. H. *Acta Crystallogr., Sect. A* **1995**, *51*, 33–38.

(27) Spek, A. L. *Acta Crystallogr., Sect. A* **1990**, *46*, C34.

(28) Sheldrick, G. M. *Acta Crystallogr., Sect. A* **1990**, *46*, 467–473.

(29) Sheldrick, G. M. SHELXL-97. A Program for the Refinement of Crystal Structures; Universität Göttingen, Göttingen, Germany, 1997.